ENGINEERING TRANSACTIONS • *Engng. Trans.* • 40, 4, 435–456, 1992
Polish Academy of Sciences • Institute of Fundamental Technological Research

STRENGTH ANALYSIS OF AXIALLY SYMMETRIC ELEMENTS WITH A SERIES OF RECTANGULAR NOTCHES

L. DIETRICH, J. MIASTKOWSKI (WARSZAWA)
and R. SZCZEBIOT (BIAŁYSTOK)

Complete solutions for axially-symmetric tensile rods with rectangular notches of arbitrary spacing are presented. On the basis of the obtained solutions both limit values of a diameter of the rod outside notch and appropriate spacings of a series of notches have been determined. Strength analysis of such elements within entire range of their geometrical parameters has also been made. The obtained results are compared with experimental tests on specimens made of aluminium alloy.

1. Introduction

Shield's method [1] to solve the plastic flow boundary value problems in the conditions of rotational symmetry has proved to be an effective tool to determine ultimate load of notched elements. The necessary system of equations for stresses comprises two equilibrium equations, Tresca's yield condition and the Haar-Kármán hypothesis whereas for plastic strain rates we have additionally the incompressibility and the isotropy conditions. This system of equations can be solved with the use of the method of characteristics, first in stresses and afterwards in strain rates. Many specific problems of plastic flow have been solved in this manner [2–8]. Some of the solutions are also collected in the monograph [10].

The solutions for stresses and strain rates in the plastic region should be completed with an extension of the stress state into neighbouring rigid regions; suitable procedure was proposed by BISHOP [9]. Such an extension is necessary to ensure that nowhere outside the plastic region the yield condition is violated. Moreover, the stress state extension provides very important practical information on the required dimensions, diameters and lengths of a considered element outside its notch. In addition, the knowledge of stress state extension into a rigid region in the case of notches having various shapes and dimensions makes it possible to rationally assess their load-carrying capacity in spite of the fact that exact solution is unattainable.

However, the extension of the stress field into a rigid region is usually more difficult and much time-consuming than determination of the stress state and strain rate state in the plastic region itself. Increased amount of time results from the fact that the rigid region is usually much bigger than the zone under yielding. Substantial difficulties also arise due to the existence of stress discontinuities, especially when the notches are rather sharp and the ultimate load factor reaches a relatively large value. This factor is defined as a ratio of the ultimate load of a notched bar to the ultimate load of a prismatic bar having a net cross-section. The discontinuity lines are a result of overlapping of different regions of characteristic nets and considerably hinder the numerical procedure for the solution of the system of equations. The stress field has so far been extended with either the use of a graphical method [5] or a numerical procedure. Solution regions have been glued together step-by-step by means of a graphical procedure in a close vicinity of the stress discontinuity line [6]. In both cases the extension proved to be very cumbersome and was usually confined to one or at most two solutions in the whole range parameters that characterized a notch under consideration.

In the paper a numerical procedure is worked out to extend the stress state into a rigid zone for rotationally symmetric rods weakened by a notch of an arbitrary shape and dimensions. The procedure is capable of recognizing an appearance of stress discontinuity line and determinig its shape. The construction of characteristic lines net in the entire rigid region can be realized in a single numerical programme written for a PC/AT compatible microcomputer. Thus, a characteristic net in the rigid zone can be found for various dimensional situations and precise dimensions of the rod outside the notch can be found as a function of the notch itself. This, in turn, makes it possible to analyse the ultimate behaviour of a rod with a number of rectangular notches and to find the right spacing between the neighbouring ones. The theoretical analysis based on the plasticity theory was not verified experimentally with the help of suitable specimens made of structural aluminium alloy.

2. Ultimate load of a rod with a single rectangular notch

The ultimate load of an axially symmetric rod with a circumferential notch of rectangular profile can be arrived at by solving the system of simultaneous equations consisting of two equilibrium equations, Tresca's

yield condition and the Haar-Kármán full plasticity hypothesis. It was R.T. SHIELD [1], who proposed to introduce two new unknowns, namely an angle ϑ included between the direction of the major principal stress and the r-axis and p, i.e. a mean value of two principal stresses σ_1, and σ_2 acting in a meridional plane. This substitution enabled the governing system of equations to reduce two partial differential equations of the hyperbolic type. Suitable characteristic equations and the compatibility equations along them have the form:

for the family α

$$\frac{dz}{dr} = \operatorname{tg}\vartheta\,, \qquad dp - 2k\,d\vartheta - \frac{k}{r}(dz - dr) = 0\,, \tag{2.1}$$

for the family β

$$\frac{dz}{dr} = -\operatorname{ctg}\vartheta\,, \qquad dp + 2k\,d\vartheta + \frac{k}{r}(dz + dr) = 0\,, \tag{2.2}$$

where z and r are the coordinate axes and k denotes the yield point in shear.

Solution for a rectangular notch with specific dimensions consists in the numerical construction of a characteristics net, starting from a degenerated characteristic problem DBE (Fig.1), determined by a point B and a line DB. In a triangle ABD we have clearly a one-dinensional tension. A curve ED determines a solution of a mixed problem in DEO. Yielding zone is bounded by a characteristic BEO through the origin of the coordinate axes and a fan angle at the point B cannot exceed $45\,°$. If an α-characteristic starting from a fan at the point B for $\vartheta = 0\,°$ (fan angle $45\,°$) will intersect the r-axis at a distance larger than the accuracy δ_r of aiming at the origin (δ_r is here assumed to be 10^{-5}), then the region of solution will be enlarged by a zone of influence of a free edge BC of the notch. Solution net is then as shown in Fig.2 in which the following additional regions can be seen: Cauchy's problem BCF, a fan FBG with an included angle of $45\,°$, characteristic problem $BGHIJE$ and mixed problem IOJ. The distance of the point C from the bottom of the notch AB is such that the α-characteristic starting from the point C hit the origin of the reference frame. Type of the characteristic net in the plastic region depends on the characteristic dimension of the notch; in the case of a rectangular one what counts is the width AB denoted either by e, or nondimensionally by β as a ratio of e the minimum diameter of the cross-section of the rod in question. The characteristic net shown in Fig.1 is valid for $\beta > 0.40608$ and is constructed

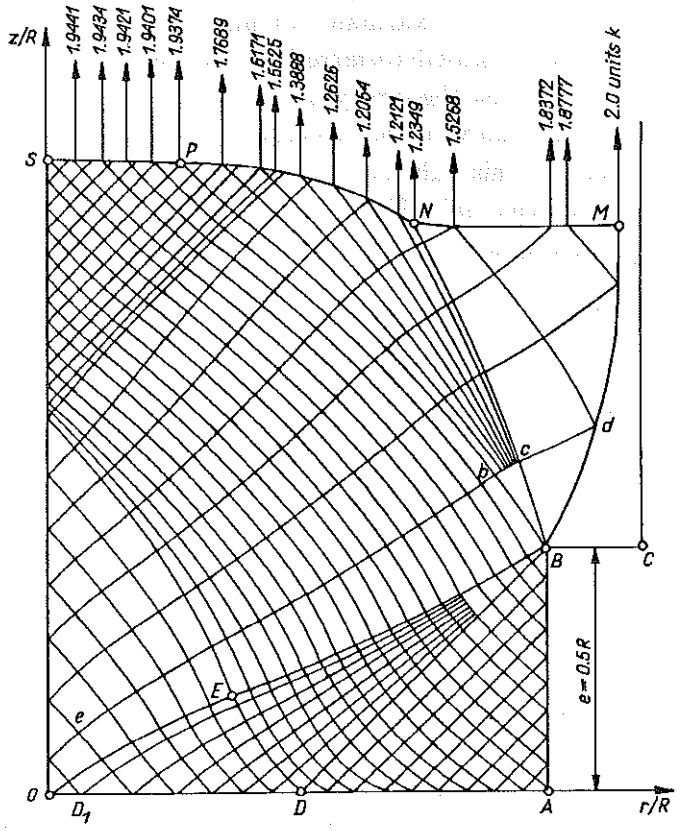

FIG. 1.

for a specific ratio $\beta = 0.5$. The other type of characteristic net, shown in Fig.2, is applicable for $\beta < 0.40608$. For an ideal ($\beta = 0$) notch the solution corresponds to that given by SHIELD [1] in which the fan included angle is equal to 90°. Once a characteristic net in the plastic region is established, the axial stresses σ_z in the minimum cross-section OA can be found and investigated over the whole area. Then the ultimate load factor f can be readily calculated as the ratio of the notched bar ultimate load capacity to that without any notch and having the diameter corresponding to the notched segment. The factor f is a nondimentional parameter describing the strength of an axially symmetric rod weakened by a rectangular notch designated by a number $\beta = e/R$.

A solution for stresses should be supplemented by a strain rate solution which enables the former to be checked by ascertaining that the power dissipated at particular nodes of the characteristic net remains positive. A proce-

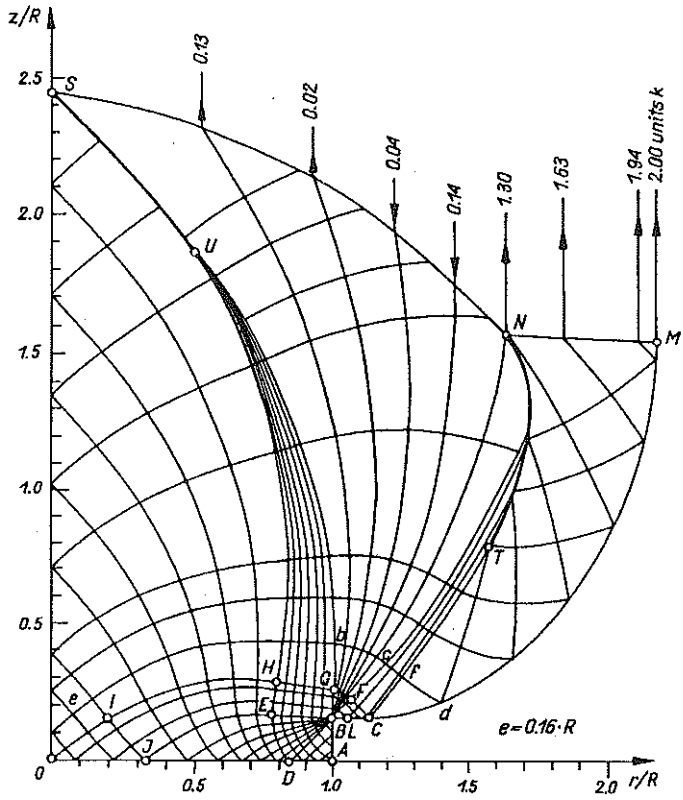

FIG. 2.

dure to determine such a strain rate field was put forward by R.T. SHIELD [1]. The starting system of equations contains the requirement of isotropy and incompressibility and turns out to be hyperbolic. In addition, the same two characteristic lines as those valid for stresses govern the plastic flow situation. The differential relationships which must be satisfied along the characteristic have now the form

$$
\begin{aligned}
dU - W\,d\vartheta &= -\frac{v_r}{2r}ds_\alpha \qquad \text{along the family } \alpha\,, \\
dW + U\,d\vartheta &= -\frac{v_r}{2r}ds_\beta \qquad \text{along the family } \beta\,,
\end{aligned}
\tag{2.3}
$$

where v_r, U, W are the strain rate components along the directions r, α, β, respectively and ds_α, ds_β are incremental segments of corresponding characteristic lines.

Boundary conditions along the characterictic BEO result from a given velocity v_0 of rigid portions of the bar in the z-direction. The solution starts

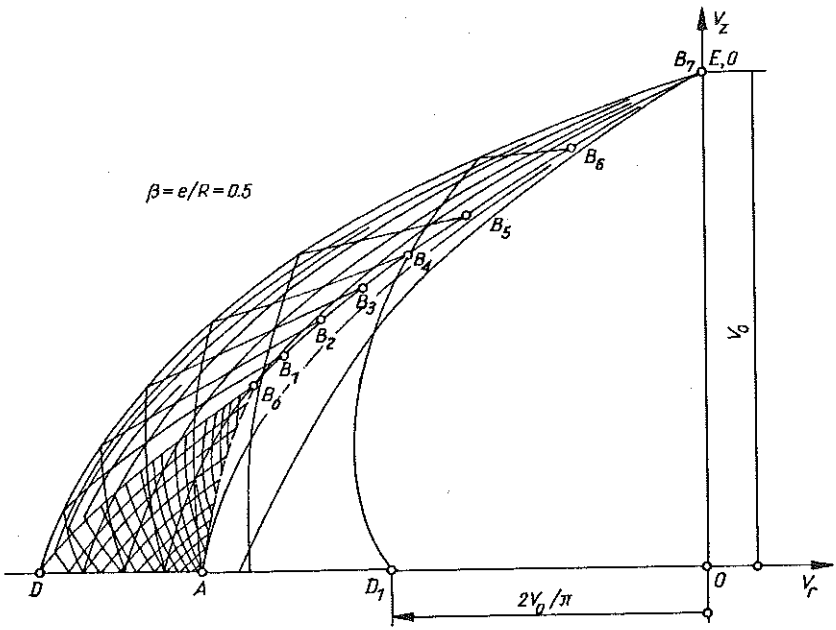

FIG. 3.

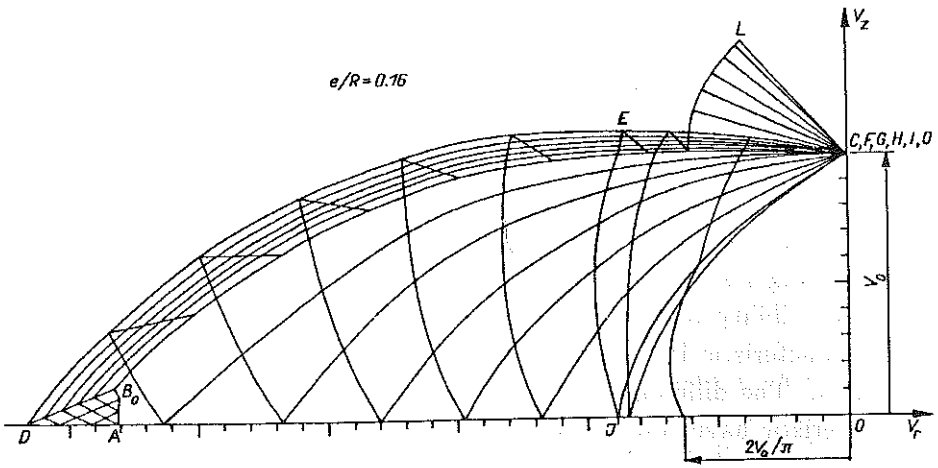

FIG. 4.

from the point D, at which the velocity $v_r = 2v_0/\pi$, see [1]. Step-by-step integration of the equation [2] leads to the velocity hodograph for all the nodal points within the yielding region. As an example, two velocity plans corresponding to two types of characteristic nets with $\beta = 0.5$ and $\beta = 0.16$ are shown in Figs.3 and 4, respectively. Dissipation power is positive for all the boundary value problems solved in the paper.

3. Extension of the stress field into rigid region

The knowledge of the stress and strain rate solutions in the plastic region constitutes an exact solution that satisfies all the static and kinematics requirements provided the dimensions of the bar beyond the notch are sufficiently large and at no other point except in the plastic region bounded by a characteristic through the origin of the coordinate axes the yield condition is violated. Extension of the stress field into a rigid zone follows a procedure devised by J.F.Bishop [9]. The solution (Fig.1) starts from a boundary characteristic BEO of the rigid region at a point lying on the symmetry axis z. Next, locations of the points of the following α-line are found by first solving the chracteristic problem (points $e-b$), the degenerated problem (points of the fan $b-c$) and an inverse Cauchy's problem (point d), Fig.1. In the case of the other type of characteristic set, the extension additionally includes the points $c-f$, Fig.2, of the characteristic problem. Solution pattern in particular extension zones is virtually arbitrary, although it appears expedient to perfom calculations for the consecutive α-lines order to minimize the tables in which the data for only one current α-line must be stored. Subsequent α-lines of the extension are determined so long as the determined free edge becomes parallel to the z-axis. Point M at which a tangent to the free edge makes 90° with the r-axis is a beginning of a statically admissible discontinuity surface $MNPS$. This surface is determined from the condition that beyond it a uniaxial tension or compression takes place. The next α-lines are found to terminate at a discontinuity line approaching the z-axis.

For sufficiently narrow notches it is possible that, starting from certain points T, U (Fig.2) in the rigid region, some stress discontinuity line may appear. To ascertain its presence a check is necessary whether the coordinates r of the next points on the d-line in question is larger than that belonging to the preceding point,

$$r[i,j-1] > r[i,j], \tag{3.1}$$

where i denotes the rumber of an α-line, j denotes the number of a β-line, increasing from the symmetry line. When the condition (3.1) is met, the calculations are continued for the subsequent points. Its violation means that the two neighbouring β-lines try to intersect each other. A procedure is now engaged to determine a statically admissible discontinuity line for stresses on both its sides. Next, consecutive points are found to fill the whole region

bounded by a line BdM of a hypothetical free edge and a stress discontinuity line $MNPS$. The coordinate r of the point M and the coordinate z of the point S determine the necessary diameter and lenght of the rigid part of the bar. Integration of the σ_z stresses above the stress discontinuity line $MNPS$ makes it possible to evaluate an accuracy of the stress state assessment by comparing this integral value with the tensile force at the notched section OA.

A complete ultimate load solution with properly specified boundary conditions consists of the construction of the characteristic net for stresses and strain rates in the plastic region $ABEO$ or $ABCGHO$, determination of the plastic flow field in the region under yielding, check on the dissipation power being greater than zero and the extension of the stress field into a rigid region. The latter operation makes it possible to find dimensions of the considered bar outside the notch necessary for the assumed yielding pattern to be realized as governed by the characteristic net at the minimum cross-section. Suitable segments of the numerical program were written in FORTRAN and the calculations were made with the help of a PC/AT microcomputer.

Table 1.

$\beta = e/R$	f	$\kappa = C/R$	$\eta = S/R$
0.0	2.8450	3.2000	3.3600
0.1	2.1434	2.5518	
0.2	1.6388	1.9208	2.1805
0.3	1.3439	1.4981	
0.4	1.1863	1.2824	
0.5	1.0975	1.1588	1.3037
0.6	1.0474	1.0858	1.1500
0.7	1.0200	1.0402	1.0922
0.8	1.0066	1.0162	1.0500
0.9	1.0011	1.0037	
1.0	1.0000	1.0000	1.0000

All the situations referring to the notch dimensions are shown in Table 1 together with the factors f, diameters C and spacing S of the notches (see

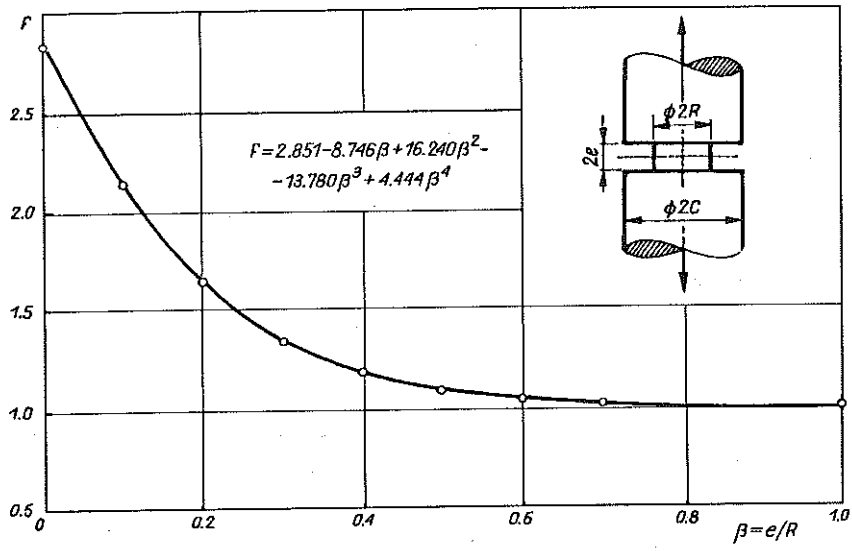

FIG. 5.

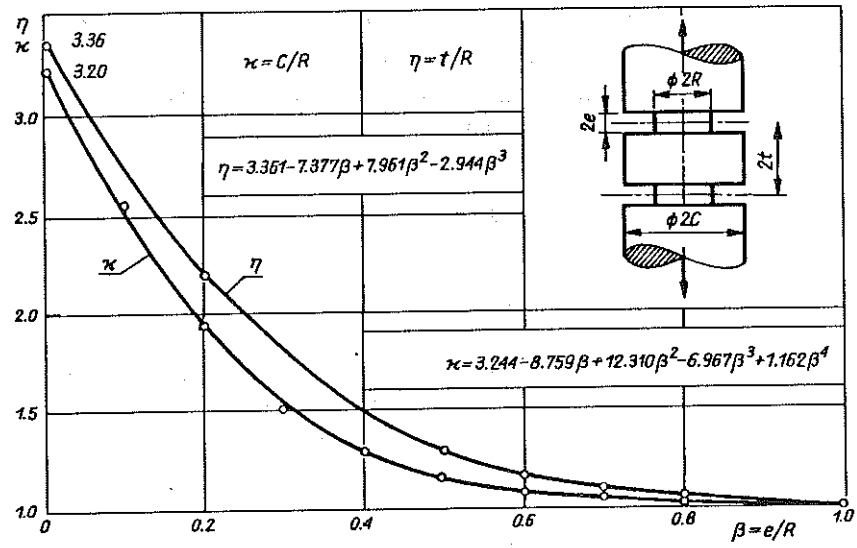

FIG. 6.

Fig.6). These three magnitudes depend on the notch dimension e. Relationship between f and a dimensionless measure of e ($\beta = e/R$) is depicted in Fig.5 in which an approximating polynomial function $f = f(\beta)$ ia also shown. Both the degree and the coefficients of the polynomial were found via the least squares method. The function is

$$f = 2.851 - 8.746\beta + 16.240\beta^2 - 13.780\beta^3 + 4.444\beta^4 . \tag{3.2}$$

In a similar way the relationships between $\kappa = C/R$ and $\eta = S/R$ as depending on a dimensionless notch width $\beta = e/R$ are given in Fig.6. These are:

for a nondimensional notch spacing

$$\eta = 3.361 - 7.377\beta + 7.961\beta^2 - 2.944\beta^3, \tag{3.3}$$

for a nondimensional bar diameter

$$\kappa = 3.244 - 8.759\beta + 12.310\beta^2 - 6.967\beta^3 + 1.162\beta^4. \tag{3.4}$$

4. Ultimate load assessment for an axially symmetric tensile bar with a series of rectangular notches

A complete solution for a single rectangular notch remains valid so long as the spacing of notches is large enough not to introduce any interacting disturbances. Such a situation is visualized in Fig.7. When the dimensions C or t are smaller than those corresponding to the stress field extension, an upper and lower assessment of the ultimate load can be furnished by making use of various solutions each valid for a single notch.

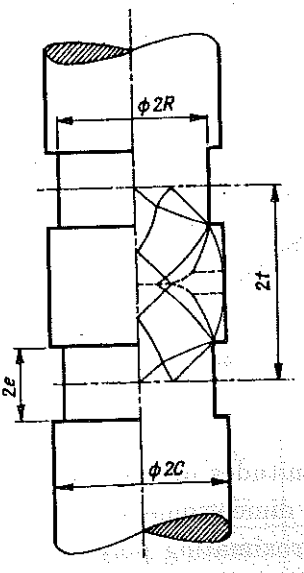

Fig. 7.

An influence of the parameter C/R on the ultimate load of a singly notched bar was investigated in a number of papers [3–5, 11] in which

a method was also given for assessing the load-carrying capacity. The obtained results remain valid for multiply notched bars provided the value of $\kappa = C/R$ is less than a certain number. Stress field extensions into a rigid region made it possible [5] to assess the tensile ultimate load for axially symmetric bars weakened by a series of V-shaped notches. Detailed analysis of results and their collection was presented in the monograph [10]. A complete solution for an axially symmetric bar with a circular notch with various radii was given in [6]. The above solutions were used later on to make a comprehensive analysis of the elements in question throughout the whole range of geometric parameters. In this paper both upper and lower ultimate load assessments are provided for a round cross-section bar with a series of rectangular notches, particular attention being paid to the specific notch width $\beta = e/R = 0.5$. An assumption was made that the diameter of a rigid part of the bar, defined by $\kappa = C/R$, is large enough. The obtained

Table 2.

L.p.	Designation	$2t$ [mm]	σ^*_{pl} [MPa]	σ^*_m [MPa]	$\eta = \frac{t}{R}$	$f = \frac{\sigma^*_{\mathrm{pl}}}{\sigma_{\mathrm{pl}}}$	$f = \frac{\sigma^*_m}{\sigma_m}$	General data
1	N1	0.0	227.0	288.10	0.000	1.201	1.150	
2	N1a	0.0	229.0	291.10	0.000	1.212	1.162	$2R_{\mathrm{sr}} =$ 8.0 [mm]
3	N2	1.0	213.0	269.09	0.125	1.127	1.074	
4	N3	2.0	205.0	259.77	0.250	1.085	1.037	
5	N4	3.0	200.0	257.09	0.375	1.058	1.026	$\sigma_{\mathrm{pl}} =$ 189.0 [MPa]
6	N5	4.0	198.0	255.58	0.500	1.048	1.020	
7	N6	5.0	204.0	262.63	0.625	1.079	1.048	
8	N7	7.0	216.0	278.02	0.875	1.143	1.109	$\sigma_m =$ 250.6 [MPa]
9	N8	10.0	225.0	287.77	1.250	1.190	1.148	
10	N9	14.0	226.0	287.45	1.750	1.196	1.147	
11	N10	18.0	226.0	292.10	2.250	1.196	1.166	$\beta = e/R =$ 0.5
12	N11	22.0	225.0	288.06	2.750	1.190	1.149	
13	N12	28.0	229.0	289.27	3.500	1.212	1.154	
14	N13	32.0	228.0	289.02	4.000	1.206	1.153	$\kappa = C/R =$ 2.0
15	N14	40.0	226.0	289.72	5.000	1.196	1.156	

assessments were referred to the ultimate load of singly notched specimens (for instance, a diagram $N1$ in Fig.13 for which, according to Table 2, the ratio $\eta = t/R$ equals zero – so does for the specimen $N1a$).

4.1. Upper bound on the ultimate load

An assessment from above is arrived at by assuming an arbitrary, kinematically admissible deformation pattern. Assuming P^* to be an exact answer, its upper bound P_g can be readily found via virtual work equation, i.e. by equating the work done by external loads to the work dissipated or an arbitrary, kinematically admissible collapse mode [12]. The ultimate load factor for a notched bar is described by a ratio

$$f = \frac{P^*}{P_0}, \tag{4.1}$$

where P_0 is a yield force for a constant cross-section bar with the diameter $2R$. Upper bound on f has the form

$$f_g = \frac{P_g}{P_0}. \tag{4.2}$$

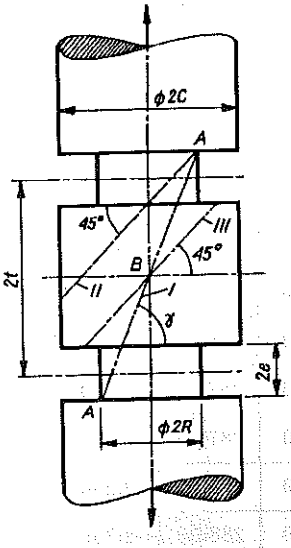

FIG. 8.

In the paper three simple shear mechanisms are admitted as shown in Fig.8. The slip plane in the mechanism I joints diagonally two points A,

each at the bottom of two adjacent notches. The angle γ is here variable and clearly depends on the spacing of notches. Upper assessment of the ultimate tensile load is obtained to be

$$(4.3)_1 \qquad f_g^{Ia} = \frac{1+(\eta+\beta)^2}{2(\eta+\beta)} \qquad \text{for} \quad 0 \le \eta \le \beta,$$

and

$$(4.3)_2 \qquad f_g^{Ib} = \frac{1+(\eta+\beta)^2}{2(\eta+\beta)}(A+B) \qquad \text{for} \quad \eta \ge \beta,$$

where

$$\begin{aligned} A &= 1+\frac{1}{90}(\kappa^2 K - L), \\ B &= \frac{2(\eta-\beta)}{\pi(\eta+\beta)}(\kappa\cos K - \cos L), \\ K &= \arcsin\frac{\eta-\beta}{\kappa(\eta+\beta)}, \\ L &= \arcsin\frac{\eta-\beta}{\eta+\beta}. \end{aligned}$$

The notation $\kappa = C/R$, $\beta = e/R$, $\eta = t/R$ was used in the above formulae as indicated in Fig.9.

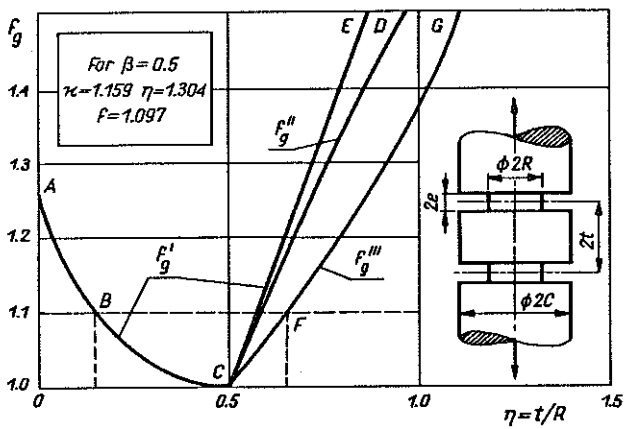

FIG. 9.

In the mechanism II, Fig.8, the slip plane starts from the point A and makes an angle 45° with the logitudinal axis of the specimen. Upper bound on the ultimate load is given by

$$(4.4)_1 \qquad f_g^{IIa} = A + B \qquad \text{for} \quad (1-\beta) \le \eta \le 1,$$

where

$$
\begin{aligned}
A &= 1+\frac{1}{180}\left[\kappa^2(K+M)-L-N\right], \\
B &= \frac{1}{\pi}\left[(1-2\beta)(\kappa\cos K-\cos L)+(2\eta-1)(\kappa\cos M-\cos N)\right], \\
K &= \arcsin\frac{1-2\beta}{\kappa}, \\
L &= \arcsin(1-2\beta), \\
M &= \arcsin\frac{2\eta-1}{\kappa}, \\
N &= \arcsin(2\eta-1),
\end{aligned}
$$

$(4.4)_2$ $$f_g^{\mathrm{IIb}} = A+B \qquad \text{for} \quad 1\le\eta\le\frac{1}{2}(\kappa+1),$$

where

$$
\begin{aligned}
A &= 0.5+\frac{1}{180}\left[\kappa^2(K+M)-L\right], \\
B &= \frac{1}{\pi}\left[(1-2\beta)(\kappa\cos K-\cos L)+\kappa(2\eta-1)\cos M\right], \\
K &= \arcsin\frac{1-2\beta}{\kappa}, \\
L &= \arcsin(1-2\beta), \\
M &= \arcsin\frac{2\eta-1}{\kappa},
\end{aligned}
$$

and

$(4.4)_3$ $$f_g^{\mathrm{IIc}} = A+B \qquad \text{for} \quad \eta\le 0.5(\kappa+1),$$

where

$$
\begin{aligned}
A &= 0.5+\frac{1}{180}\left[\kappa^2(90+K)-L\right], \\
B &= \frac{1}{\pi}\left[(1-2\beta)(\kappa\cos K-\cos L)\right], \\
K &= \arcsin\frac{1-2\beta}{\kappa}, \\
L &= \arcsin(1-2\beta).
\end{aligned}
$$

The mechanism III is formed by a slip plane passing through the point B and inclined at 45°. The upper bound here is

$(4.5)_1$ $$f_g^{\mathrm{IIIa}} = A+B \qquad \text{for} \quad (1-\beta)\le\eta\le(1+\beta),$$

where

$$A = \frac{1}{90}(\kappa^2 K + L),$$
$$B = \frac{2(\eta-\beta)}{\pi}(\kappa \cos K - 2\sin L),$$
$$K = \arcsin\frac{\eta-\beta}{\kappa},$$
$$L = \arccos(\eta-\beta),$$

$(4.5)_2$ $$f_g^{\mathrm{III}b} = A + B \quad \text{for} \quad (1+\beta) \le \eta \le (\kappa+\beta),$$

where

$$A = \frac{2}{\pi}(\eta-\beta)\sqrt{\kappa^2-(\eta-\beta)^2},$$
$$B = \kappa^2\left(1 - \frac{1}{90}\arccos\frac{\eta-\beta}{\kappa}\right),$$

and

$(4.5)_3$ $$f_g^{\mathrm{III}c} = \kappa^2 \quad \text{for} \quad \eta \ge (\kappa+\beta).$$

For known dimension of the element and given notch characteristic $2e$ the above formulae became much simpler. The above obtained solutions were subject to experimental verification on notched samples with the following dimensions: $\kappa = C/R = 2.0$, $\beta = e/R = 0.5$. The derived general formuale take the specific forms:

Instead of (4.3) we have:

$(4.6)_1$ $$f_g^{\mathrm{I}a} = \frac{\eta^2+\eta+1.25}{2\eta+1} \quad \text{for} \quad 0 \le \eta \le 0.5,$$

and

$(4.6)_2$ $$f_g^{\mathrm{I}b} = \frac{\eta^2+\eta+1.25}{2\eta+1}(A+B) \quad \text{for} \quad \eta \le 0.5,$$

where

$$A = 1 + \frac{1}{90}(4K - L),$$
$$B = \frac{2\eta-1}{\pi(\eta+0.5)}(2\cos K - \cos L),$$
$$K = \arcsin\frac{\eta-0.5}{2\eta+1},$$
$$L = \arcsin\frac{\eta-0.5}{\eta+0.5}.$$

Instead of Eqs.(4.4) we get:

$$(4.7)_1 \qquad f_g^{\mathrm{IIa}} = A + B \qquad \text{for} \quad 0.5 \leq \eta \leq 1\,,$$

where

$$\begin{aligned} A &= 1 + \frac{1}{180}(4M - N)\,, \\ B &= \frac{1}{\pi}[(2\eta - 1)(2\cos M - \cos N)]\,, \\ M &= \arcsin\frac{2\eta - 1}{2}\,, \\ N &= \arcsin(2\eta - 1)\,. \end{aligned}$$

$$(4.7)_2 \qquad f_g^{\mathrm{IIb}} = A + B \qquad \text{for} \quad 1 \leq \eta \leq 1.5\,,$$

where

$$\begin{aligned} A &= 0.5 + \frac{1}{45}M\,, \\ B &= \frac{1}{\pi}[2(2\eta - 1)\cos M]\,, \\ M &= \arcsin\frac{2\eta - 1}{2}\,, \end{aligned}$$

and

$$(4.7)_3 \qquad f_g^{\mathrm{IIc}} = 2.5 \qquad \text{for} \quad \eta \geq 1.5\,.$$

Instead of Eqs.(4.5) we obtain

$$(4.8)_1 \qquad f_g^{\mathrm{IIIa}} = A + B \qquad \text{for} \quad 0.5 \leq \eta \leq 1.5\,,$$

where

$$\begin{aligned} A &= \frac{1}{90}(4K - L)\,, \\ B &= \frac{2(\eta - 0.5)}{\pi}(2\cos K - 2\sin L)\,, \\ K &= \arcsin\frac{\eta - 0.5}{2}\,, \\ L &= \arccos(\eta - 0.5)\,. \end{aligned}$$

$$(4.8)_2 \qquad f_g^{\mathrm{IIIb}} = A + B \qquad \text{for} \quad 1.5 \leq \eta \leq 2.5\,,$$

where

$$A = \frac{2}{\pi}(\eta - 0.5)\sqrt{3.75 + \eta - \eta^2}\,,$$
$$B = 4\left(1 - \frac{1}{90}\arccos\frac{\eta - 0.5}{2}\right),$$

and

$$(4.8)_3 \qquad f_g^{\mathrm{IIIc}} = 4 \qquad \text{for} \quad \eta \geq 2.5\,.$$

The relationships (4.6), (4.7) and (4.8) are persented diagrammatically in Fig.9. It can be readily seen that the best, i.e. the lowest, upper bound for the worked out example is associated with the mechanism I for $0 \leq \eta \leq 0.5$ (line AC) and with the mechanism III for $\eta \geq 0.5$ (line CG). For a bar having a rectangular notch with $\beta = 0.5$, the ultimate load factor resulting from the complete solution amounts to $f = 1.0975$ and is shown in Fig.9 by a horizontal broken line. It intersects the curve AC at B and the curve CG at F. The coordinate η of the point B is found to be

$$(4.9) \qquad \eta^2 + (2\beta - 2.195)\eta + \beta^2 - 2.195\beta + 1 = 0\,.$$

For a particular value $\beta = 0.5$ it assumes the form of a standard quadratic equation

$$\eta^2 - 1.195\eta + 0.1525 = 0\,,$$

whose meaningful root supplies the sought value $\eta_B = 0.1453$. The value of f_g^{IIIa} for the point F equals 1.0975. Inserting $\beta = 0.5$ into Eq.$(4.8)_1$ yields $\eta_F = 0.65085$. Upper bound on the ultimate load for $0 \leq \eta < 0.1453$ is associated with a single notch bar having $\beta = 0.5$. Ultimate load within this range is certainly larger than the complete answer for a bar provided with two notches.

It is worth remembering that for $\eta = 1.304$ there exists an exact solution. It is only for $\eta \geq 1.304$ that we have an exact value of the ultimate load factor $f = 1.0975$, whereas for η between $\eta_F = 0.65085$ and 1.304 we obtain only an assessment.

4.2. Lower bound on the ultimate load

For $1 < \eta = t/R < 1.304$ a lower bound for a rectangularly notched bar with $\beta = e/R$ was assumed to be equal to that corresponding to such a

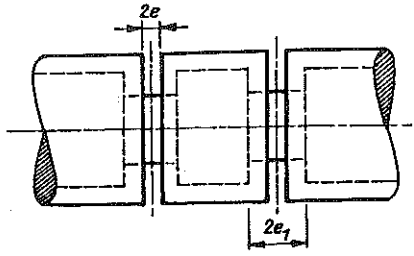

FIG. 10.

notch width $2e$, for which a complete solution can be found (corresponding bar is shown in Fig.10 by broken line). For $0 < \eta < 1$ a lower bound was determined by plotting a rectangular notch $2e$ wide and reaching on outer circumference of the bar, see Fig.11. The ultimate load of a bar weakened by such a single notch constitutes a lower assessment for a bar with closely spaced notches and, at the same time, represents a solution for a single notch provided the parameter η decreases to reach $\eta = \beta$, and thus the width of a middle part, separating the two notches, completely vanishes and only one notch $2e$ wide remains.

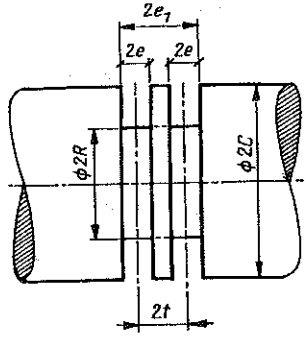

FIG. 11.

5. TEST RESULTS

Experimental verification of the presented exact and approximate solutions was made with the use of axially symmetric bars each having two circumferential rectangular notches done by turning. 17 specimens were tested (two unnotched ones were used for standard uniaxial test). Aluminium alloy PA 2(AlMg 2) was selected as having very distinct plastic properties and as

a widely used structural material to manufacture various parts in the aircraft and construction industry as well as in naval architecture, chemistry and food processing. Relevant shapes and dimensions are shown in Fig.12. Minimum diameter $2R$ at the bottom of a notch was assumed to be constant for all testpieces and so was the notch width $2e$. Average value of the parameter $\beta = e/R$ (neglecting some tolerances) was 0.5 whereas the parameter $\kappa = c/R$ was taken to be 2.0. Thus the latter value was greater than that assumed in theoretical solutions (for $\beta = 0.5$ it amounted to 1.159, cf. Fig.6 and Table 1).

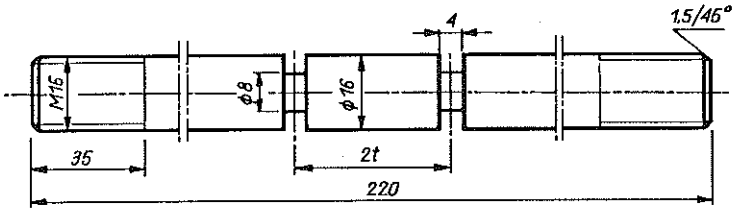

FIG. 12.

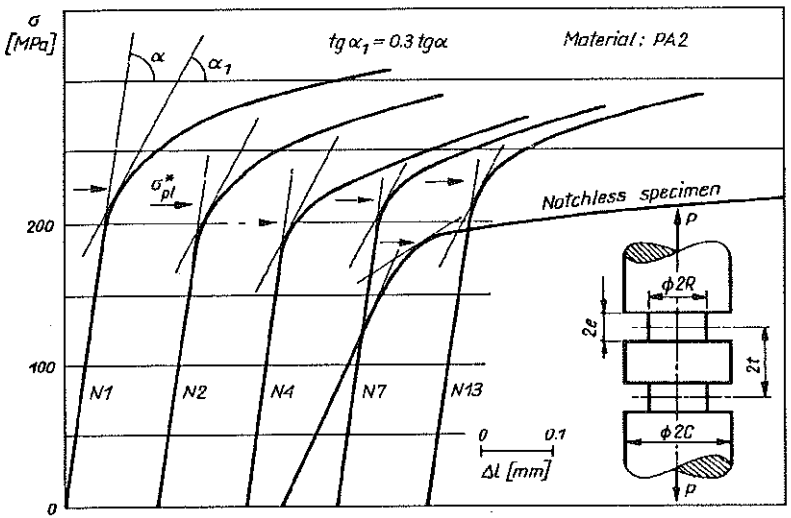

FIG. 13.

Spacing $\eta = t/R$ is given in Table 2, different for each specimen and contained within the range $0 \div 5$.

Tests were performed on a universal hydraulically-driven testing machine. To avoid unnecessary bending, spherical hinge, were used. Strains were measured with the use of an AMSLER mechanical extensometer whose minimum

division was 0.01 mm and the base was 120 mm. A number of initial tensile curves are shown in Fig.13. Nominal yield points are shown with the help of arrows. These were determined by identifying points at the tensile diagrams whose slopes were 0.3 of the initial straight part slope of the diagram. Relevant values are given in Table 2. These yield stresses are also shown in Fig.14 by small circles thus visualizing an influence of notch spacing $\eta = t/R$ on the nominal yield stress. Theoretical value of the parameter $\eta_t = 1.304$ is shown by broken line. It corresponds to the solution for $\beta = 0.5$ (Table 1 and Fig.6). Location of circles in Fig.14 that, as mentioned before, indicate the yielding of notched specimens show that for notch spacing $2t$ smaller than the theoretical spacing for $\eta \leq \eta_t = 1.304$ an initially smooth and then more abrupt decrease of the ultimate load can be observed. The smallest load-carrying capacity corresponds to $\eta = 0.5$. For further decrease in notch spacing (for $\eta < 0.5$) an increased ultimate load is observed reaching the value associated with a bar weakened by a single notch ($\eta = 0$). A decrease in the ultimate load is accompanied by a change in the collapse mechanism. Specimens with η larger than the theoretical one split in one of the notches whereas for the specimens with $0 < \eta < \eta_t$ the collapse was taking place on the surface between the notches. Theoretical assessments obtained before are shown in Fig.14 by solid lines.

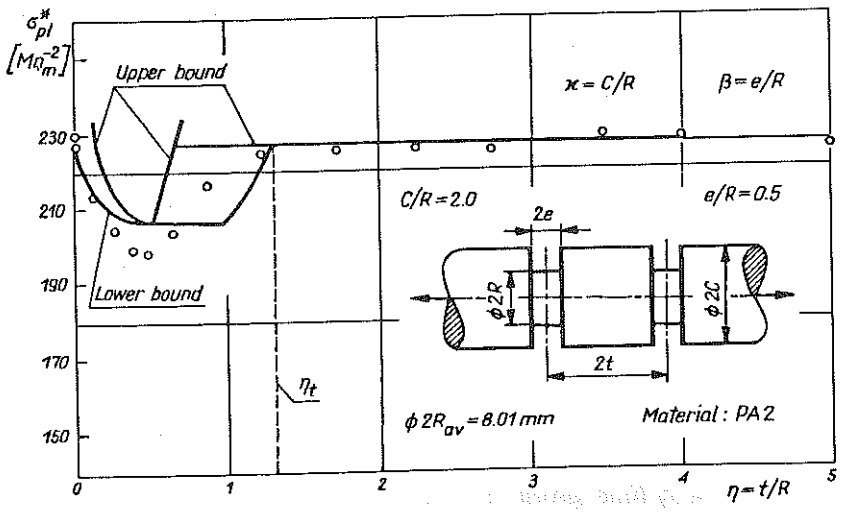

FIG. 14.

The tension process of the specimens was continued up to failure and the tensile strength was duly registered. Tensile strength σ^*_m as a function

of the dimensionless notch spacing $\eta = t/R$ is shown in Fig.15. Similarly as for the ultimate load (Fig.14) a distinct drop in the tensile strength is observed for $\eta = t/R$ smaller than the theoretical value $\eta_t = S/R = 1.304$. Miniumum strength occurs for $\eta = 0.5$. Due to further decrease of the notch spacing the tensile strength begins to grow to eventually reach the strength of a specimen with a single notch, $\eta = 0$.

6. Conclusions

The obtained diagrams of the optimum geometrical parameters $\kappa = c/R$ and $\eta = s/R$ as depending on the notch characteristics $\beta = e/R$ (Fig.6) together with the diagram of the load factor f (Fig.5) make it possible to readily select suitable dimensions of axially symmetric elements with rectangular notches of various sharpness and ensure their adequate strength.

The reported tests corroborated the suitability of the proposed theoretical predictions on how to space optimally the notches to ascertain the best tensile resistance of multiply notched pieces, (Fig.15).

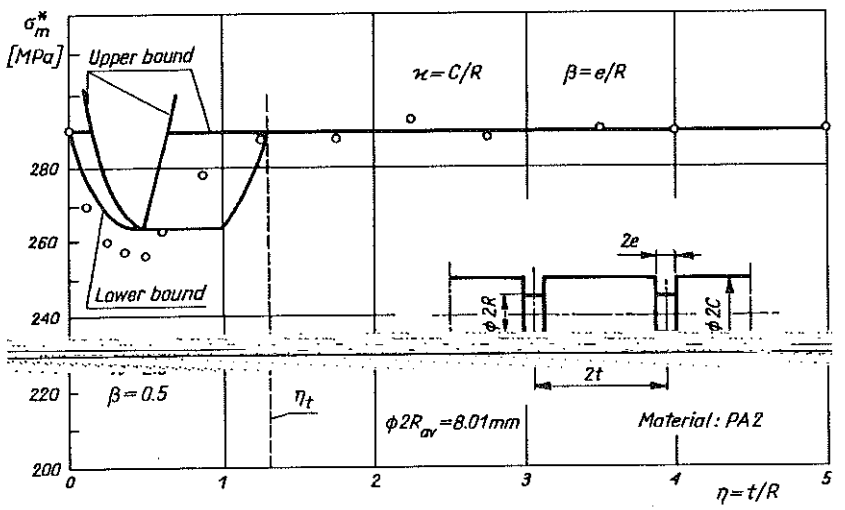

Fig. 15.

For $0 < t/R \leq \eta_{\min}$, where $\eta_{\min}$ denotes a theoretical value for a notch characterized by $\beta = e/R$, see Fig.6, it is only an evaluation of the upper and the lower bound that is at all possible as shown in the paper.

The applied procedure, similar to that put forward in [5] for axially symetric bars with V-shaped notches and checked in the paper [6] for round elements with a series of circular notches, has been here confirmed in the case of elements with a number of rectangular notches. The procedure is thus suitable for a simple determination of proper dimensions and ultimate loads for round structural elements with a series of notches of arbitrary profiles.

REFERENCES

1. R.T.SHIELD, *On the plastic flow of metals under conditions of axial symmetry*, Proc. Roy. Soc., **233A**, 1193, 267–287, 1955.
2. G.EASON, R.T.SHIELD, *The plastic indentation of a semi-infinite solid by a perfectly rough circular punch*, ZAMP, **11**, 33–42, 1960.
3. W.SZCZEPIŃSKI, L.DIETRICH, E.DRESCHER and J.MIASTKOWSKI, *Plastic flow of axially-symmetric notched bars pulled in tension*, Int. J. Solids Structures, **2**, 543–554, 1966.
4. L.DIETRICH, W.SZCZEPIŃSKI, *Plastic yielding of axially-symmetric bars with non-symmetric V-notch*, Acta Mechanica, **4**, 230–240, 1967.
5. L.DIETRICH, K.TURSKI, *Tensile ultimate load of axially-symmetric rods weakened by a number of V-shaped notches* [in Polish], Mech. Teoret. Stos., **4**, 6, 437–448,1968.
6. L.DIETRICH, J.MIASTKOWSKI, R.SZCZEBIOT, *Tensile ultimate load of axially symmetric rods with a series of circular notches* [in Polish], Rozpr. Inż., **36**, 3, 441–459, 1988.
7. F.J.LOCKETT, *Indentation of a rigid-plastic material by a conical indenter*, J. Mech. Phys. Solids, **11**, 345–355, 1963.
8. DAO-DUY TIEN, *Rockwell hardness test as a problem in plasticity* [in Polish], Rozpr. Inż., **21**, 4, 709–721, 1973.
9. J.F.BISHOP, *On the complete solution to problems of deformation of a plastic-rigid material*, J. Mech. Phys. Solids, **2**, 43–45, 1955.
10. L.DIETRICH, J.MIASTKOWSKI, W.SZCZEPIŃSKI, *Ultimate limit load of structural elements* [in Polish], PWN, Warszawa 1970.
11. J.MIASTKOWSKI, *Tensile ultimate load of notched elements with square cross-sections* [in Polish], Rozpr. Inż., **17**, 4, 571–582, 1969.
12. D.C.DRUCKER, H.J.GREENBERG, W.PRAGER, *Extended limit design theorems for continuous media*, Quart. Appl. Math., **9**, 381–389, 1952.

POLISH ACADEMY OF SCIENCES,
INSTITUTE OF FUNDAMENTAL TECHNOLOGICAL RESEARCH, WARSZAWA.

Received January 24, 1992.